Hindawi
Discrete Dynamics in Nature and Society
Volume 2020, Article ID 1382415, 11 pages
https://doi.org/10.1155/2020/1382415

Research Article

Control Strategy of Signal Transition after Emergency Vehicle Signal Preemption

Haibo Mu, Linzhong Liu, Yubo Song, and Na Wang

School of Traffic and Transportation, Lanzhou Jiaotong University, Lanzhou 730070, Gansu, China

Correspondence should be addressed to Haibo Mu; mhbmmm@mail.lzjtu.cn

Received 18 August 2019; Revised 25 October 2019; Accepted 14 November 2019; Published 27 January 2020

Academic Editor: Ewa Pawluszewicz

Emergency vehicle (EV) plays an important role in evacuations or rescues when emergencies occur. To insure that an EV can transfer people in danger to emergency shelters or medical assistance organizations as soon as possible, EV signal preemption (EVSP) strategy is usually adopted. After EV has passed through the intersection, traffic signal has to transfer back to normal signal timing scheme. This paper focuses on the control strategy of EV signal transitioning from EVSP back to normal operation. Considering both efficiency and fairness, the maximum vehicles passing through in per unit time during the transition period and the minimum difference between the maximum and the minimum queue length after transition are selected as objectives, and a multi-objective optimization model is presented. A nondominated sorting genetic algorithm II (NSGA-II) is designed to solve the optimization model and unique encoding and decoding methods are presented. The established model and designed algorithm are verified and the control effect is analyzed. Simulation results indicate that by adopting the control strategy obtained by the presented model, the number of vehicles passing through in per unit time during the transition period is increased and the difference of vehicle length in different directions is reduced significantly, from which we can conclude that the control method proposed in this paper has good performance.

1. Introduction

In modern society, emergency events, such as natural disasters, accident disasters, public health incidents, and social security incidents occur frequently and bring huge losses to people's lives and property security. Since emergency vehicle (EV) plays an important role in evacuation and rescue, it is hoped that it can reach the rescue or medical sites as soon as possible. However, the traffic congestion prevailing in modern society makes it difficult for EVs to reach their destination quickly and safely. Moreover, the operation of EV may further aggravate traffic congestion and even lead to new accidents such as vehicle collisions at intersections. In order to effectively reduce the response time of EV, improve the efficiency of emergency traffic and emergency rescue, and ensure that the EV pass through intersections safely and rapidly, EV signal preemption (EVSP) strategies have been put forward. Since EVSP was first suggested in 1929, the concept of it is not new [1]. Thanks to the development and application of Intelligent Transportation System (ITS), EVSP problems can now be dealt with in real time [2–10].

After the EV has passed through the intersection, traffic signal has to transfer from EVSP back to normal operation in a safe and expedient manner. However, most of the existing researches on signal transition schemes aim at nonemergency situations, and mainly focus on the transition from one timing plan to another so as to adapt to the change of traffic flow. When the signal control scheme changes, it is necessary to determine the transition scheme between the old and the new control schemes so as to realize the reasonable transition between different schemes in different time periods and ensure the smooth operation of traffic flow. The suppliers of traffic signal controller and the developers of traffic simulation software CORSIM have developed a series of practical methods to achieve the transitions of signal planning control. Although they use different names in different controller vendors, these methods can usually be divided into dwell, add, subtract, shortway, immediate, two-cycle and three-cycle. However, the classical algorithms mentioned above cannot meet the demand of real-time changing traffic conditions, and result to some deficiencies in signal control effect. In order to evaluate the performance of the above transition methods, some scholars

carried out simulation studies and obtained the advantages, disadvantages and applicable conditions of various methods [11–15]. In addition to the classical methods mentioned above, some scholars used prewritten transition algorithms to control signal transition process [16–18]. Other scholars studied this problem by establishing optimization models. To obtain the optimal timing scheme, they constructed performance functions to seek the optimum performance indexes during signal transition period, most of which were the shortest transition time or the least impact on social vehicles [19–24].

However, the transition strategy of how to transfer traffic signal back to normal signal after EV signal preemption is not well researched. Obenberger et al. [25] evaluated the effect of four commonly used transition strategies to illustrate which strategy can exit preemption control and switch back to normal signal timing scheme most effectively. To determine how to choose the best coordinated recovery strategy at the end of signal preemption so as to minimize the interference to normal signal operation, Yun et al. [26] employed hardware-in-the-loop simulation to study signal preemption problem and obtained the evaluation results of various EV preemption strategies for EVs arriving in a single way in coordinated traffic signal system. However, both of them mainly focused on analyzing the effect of various commonly used transition strategies, and effective signal preemption strategies were not put forward. Qin [27] proposed two signal preemption control strategies to shorten the response time of EVs. The first one was adopted to enable signal transitioning from normal operation to EVSP, and the second one, implemented by an optimal control algorithm, was used for the signal transitioning from the EVSP back to normal operation. Yao et al. [28] proposed a multi-objective signal recovery transition optimization model of emergency traffic based on power function and solved it by genetic algorithm. However, the goal of the second transition stage was to make the queue length of each line after EV passing through the intersection to not exceed the queue length under normal operation, and the other indexes, such as the number of passing vehicles, or the equilibrium or fairness of vehicles in all directions, were not considered.

As can be seen from the literatures mentioned above that nowadays few studies have focused on the problem of how to make EVs transfer back to normal signal timing scheme, and the effects of various commonly used transition strategies on exit signal preemption are emphatically analyzed. Model optimization method adopted to solve this problem is even fewer, and the objective function is either the shortest queue length or the shortest time to complete the signal transition in most cases. Therefore, this paper focuses on the optimization model method to study the control strategy of EV signal transitioning from EVSP back to normal operation. We believe that as long as the number of vehicles passing through the system in all directions during the transition period is large enough and the efficiency of the system is high enough, a slightly longer transition time has little impact on the system in fact. What is more, the equilibrium of different directions is also considered in this paper so as to obtain sufficiently small difference between the numbers of vehicles queued in all directions at the end of the transition period. The maximum numbers of vehicles passing through the system per unit time during the transition period and the minimum difference between the maximum and the minimum length after the transition are selected as the objectives, and a multi-objective signal transition optimization model is presented. An optimization algorithm based on Nondominated sorting genetic algorithm II (NSGA-II) is designed to solve the optimization model to obtain the optimal signal transition strategy.

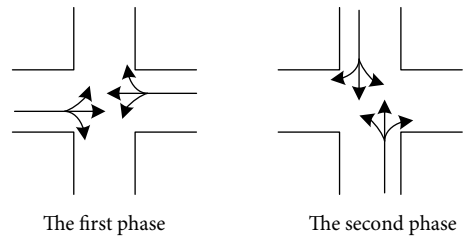

Figure 1: Phase diagram of traffic signal.

The goal of this research is to develop and evaluate a signal transition strategy based on model optimization method. We limit the scope of this paper to signal transition strategy from the EVSP back to normal operation, and the strategy from normal operation to EVSP will not be discussed further in this paper. In support of this goal, the research will seek to achieve the following objectives: (1) develop a new transition method based on a multi-objective optimization model, (2) design a solving algorithm for the presented optimization model, and (3) carry out simulation calculation and verify the efficiency of the proposed signal transition strategy.

The remainder of the paper is organized as follows. Firstly, some related time parameters are calculated in Section 2. Secondly, a multi-objective programming model for traffic signal transitioning from the EVSP back to normal operation is presented in Section 3. The NSGA-II algorithm for solving the proposed transition model is investigated in Section 4. Finally, simulation analysis is carried out in Section 5 and conclusions are presented in Section 6.

2. Calculation of Related Time Parameters

Suppose that all the intersections in the traffic network are typical four-leg intersections and controlled by two-phase signal with fixed normal cycle length, as shown in Figure 1.

For the intersection discussed in this paper, we employ ws_0, d_1 and d_2 to denote the starting time of the first phase, the duration time of the first phase and the duration time of the second phase, respectively. Suppose that EV passes through or clears intersection at time t_0. If ws_0, d_1 and d_2 are determined, then the current phase j and the elapsed green time of phase j can be calculated correspondingly. Provided that C denotes the cycle length of the intersection, and then we have:

$$D_0 = 0, \quad D_j = \sum_{k=1}^{j} d_k, \quad j = 1, 2, \tag{1}$$

$$a = \frac{(t_0 - ws_0)}{C}, \quad b = (t_0 - ws_0) \bmod C, \tag{2}$$

where mod is a function whose result is the remainder of $(t_0 - ws_0)$ divided by C. If it satisfies that $D_{u,i-1} \le b < D_{u,i}$, then the current phase is j and the elapsed green time of phase j is

$t_0 - ws_0 - a \times C - \sum_{k=0}^{j-1} D_k$, and the remaining cycle time can be denoted by $R_C = C - b$.

Let t_{safe} be the safety time interval that must be kept between the last vehicle in the queue on the EV approach and the EV so as to avoid collision between EV and social vehicles. The time duration of transition, denoted by R_d, can be written as:

$$R_d = [R_C + nC - t_{\text{safe}}], \quad n = 0, 1, 2, \ldots, \tag{3}$$

where n stands for the number of additional normal cycles so as to realize the objectives given in the next section. To avoid too long transition time, the maximum value of n is set to 3, that is to say, at most three additional signal cycles can be added.

In order to obtain EVSP signal control strategy, R_d is divided into N time steps on average, and the length of each time step, denoted by T, can be expressed as follows:

$$T = \frac{R_d}{N} = \frac{[R_C + nC - t_{\text{safe}}]}{N}. \tag{4}$$

Each time step T is the combination of green time and yellow time or there is only green time in T. If there is no signal switchover in T, then T contains at most only one yellow time. Otherwise, it is stipulated that only one signal switchover can occur in T, and T contains two or one yellow time.

Assume that there exists no all red time for traffic signal at each intersection. Let $g_{j(k)}, Y_{j(k)}$ be the green time and yellow time of phase j at time step k, respectively; and $\alpha_{j(k)}$ be a 0-1 variable, where $\alpha_{j(k)} = 1$ indicates that a signal switchover occurs in phase j at time step k and $\alpha_{j(k)} = 0$ otherwise. Then, we have:

$$\begin{aligned} NT &= [R_C + nC_i - t_{\text{safe}}] \\ &= \sum_{k=1}^{N} \left(g_{1(k)} + g_{2(k)} + Y_{1(k)} \times \alpha_{1(k)} + Y_{2(k)} \times \alpha_{2(k)}\right). \end{aligned} \tag{5}$$

In the following optimization model, we will determine the value of $g_{j(k)}$ and $\alpha_{j(k)}$ to obtain the Pareto optimal solution.

3. The Multi-Objective Transition Optimization Model

Let $q_f(k)$ be the queue length in direction f at the beginning of time step k at each intersection, $f = 1, 2, 3, 4$; $a_f(k)$ be the number of vehicles arriving in time step k, $f = 1, 2, 3, 4$; $f = 1, 2, 3, 4$ represents the direction from west to east, from east to west, from north to south and from south to north, respectively. If $q_{f-t}(k), q_{f-r}(k)$, and $q_{f-l}(k)$ denotes the number of vehicles going straight, turning right and turning left in $q_f(k)$, respectively, then we have:

$$q_f(k) = q_{f-t}(k) + q_{f-r}(k) + q_{f-l}(k), \quad f = 1, 2, 3, 4. \tag{6}$$

Let A_{f-t}, A_{f-r} and A_{f-l} be the proportion of straight, right-turn, and left-turn vehicles in direction f, respectively; S^i_{gf} and $S^i_{yf}, i = t, r, l$ be the saturation discharge rate during green time and yellow time for straight, right-turn, and left-turn vehicles in direction f, respectively; $g_{j\min}$ and $g_{j\max}$ be the minimum and maximum green time of phase j, respectively.

The proposed transition model includes two important decision variables that control the transition process. The first decision variable is a 0-1 variable $\alpha_{j(k)}$, which can be determined dynamically according to traffic condition. The second decision variable is $g_{j(k)}$, denoting the green time of phase j during time step k.

The first objective is to maximize the number of vehicles passing through the intersection in unit time during the transition period, which is the sum of the number of vehicles going straight, turning right and turning left in four directions in the green interval and yellow interval of all time steps. The second objective, which is measured at the end of the transition period, is to minimize the difference between the largest and the smallest queue length in all directions at the end of the transition period. The number of queued vehicles in each direction is composed of straight, right-turn and left-turn vehicles. If the number of straight, right-turn and left-turn vehicles in direction f at the beginning of time step k is known, then the queue length of subsequent time step $k+1, k+2, \ldots, N$ can be calculated. Taking time step $k+1$ as an example, we have

$$\begin{aligned} q_{f-i}(k+1) = {} & q_{f-i}(k) + a_f(k) \times A_{f-i} - \min\big(q_{f-i}(k) + a_f(k) \\ & \times A_{f-i}, S^i_{gf} \times g_{i(k)} + S^i_{yf} \times Y_{j(k)} \times \alpha_{j(k)}\big) \\ & k = 0, 1, 2, \ldots, N-1, \ i = t, r, l. \end{aligned} \tag{7}$$

At the end of time step N, the queue length in direction f is as follows:

$$q_f(N) = q_{f-t}(N) + q_{f-r}(N) + q_{f-l}(N). \tag{8}$$

If $q_{\max}, q_{\min}$ be the maximum and minimum value of $q_f(N)$, then the second objective function can be obtained by calculating the difference between $q_{\max}$ and $q_{\min}$.

As a multi-objective optimization model, the proposed signal transition optimization model is as follows:

$$\textit{Maximize} \quad \frac{\left\{\sum_{f=1}^{4}\sum_{k=1}^{N}\sum_{j=1}^{2}\left[\left(S^t_{gf} + S^r_{gf} + S^l_{gf}\right) \times g_{j(k)} + \left(S^t_{yf} + S^r_{yf} + S^l_{yf}\right) \times Y_{j(k)} \times \alpha_{j(k)}\right]\right\}}{R_d}, \tag{9}$$

$$\begin{aligned} \textit{Minimize} \quad & \left\{\max\left\{q_f(N+1), f = 1, 2, 3, 4\right\}\right. \\ & \left. -\min\left\{q_f(N+1) | f = 1, 2, 3, 4\right\}\right\}. \end{aligned} \tag{10}$$

Subject to:

$$\begin{aligned} q_{f-i}(k+1) = {} & q_{f-i}(k) + a_f(k) \times A_{f-i} - \min\big(q_{f-i}(k) + a_f(k) \\ & \times A_{f-i}, S^i_{gf} \times g_{j(k)} + S^i_{yf} \times Y_{j(k)} \times \alpha_{j(k)}\big) \\ & k = 0, 1, 2, \ldots, N-1, i = t, r, l, \end{aligned} \tag{11}$$

$$q_f(k+1) = \sum_{i=t}^{l} q_{f-i}(k+1), \quad k = 0, 1, 2, \ldots, N-1, \tag{12}$$

$$\sum_{k=1}^{N} T_k = R_C + nC_i - t_{\text{safe}}, \tag{13}$$

$$T_k = g_{1(k)} + g_{2(k)} + Y_{1(k)} \times \alpha_{1(k)} + Y_{2(k)} \times \alpha_{2(k)}, \quad k = 0, 1, 2, \ldots, N-1, \tag{14}$$

$$g_{j\min} \le g_{j(k)} \le g_{j\max}, \quad j = 1, 2, \tag{15}$$

$$g_{1\min} + g_{2\min} + Y_{1(k)} + Y_{2(k)} \le T_k \le g_{1\max} + g_{2\max} + Y_{1(k)} + Y_{2(k)}, \quad k = 0, 1, 2, \ldots, N-1. \tag{16}$$

In the above optimization model, Equations (9) and (10) are the objective functions. Equation (9) represents maximizing the number of vehicles passing through the intersection in unit time during the transition period, which is the quotient of the sum of vehicles going straight, turning right and turning left in four directions in the green interval and yellow interval in N time steps divided by the time duration of transition. Equation (10) represents minimizing the difference between the largest and the smallest queue length in all directions at the end of the transition period. Equations (11) and (12), namely the first and second constraint equations, denote the calculation method of straight, right-turn and left-turn queue length in each direction, and the calculation method of total queue length in each direction. Equation (13) ensures that the sum of all time steps equal to the time duration of transition. Equation (14) defines the calculation method of the green interval of time step k. Equations (15) and (16) denotes the range of the green time of phase j at time step k and that of the length of each time step k.

4. Design of Solving Algorithm Based on NSGA-II

Many evolutionary optimization methods have been used to solve multi-objective optimization problems, such as multi-objective genetic algorithm (MOGA), multi-objective differential evolution algorithm (MODEA) and nondominated sorting genetic algorithm II (NSGA-II), etc. [29]. NSGA-II adopts an elite strategy to accelerate the convergence speed. The proposed crowding distance sorting can better guarantee the diversity of the population, and the adoption of fast nondominated sorting method reduces the time complexity [30]. In order to improve the solving efficiency, NSGA-II algorithm is adopted in this paper to solve the established multi-objective optimization model.

Let $T_{\min}$ be the minimum step size during the signal transition. Let n take values from 1 to 3, respectively. If we have known the value of R_C, we can calculate the value of time duration R_d according to Equation (3). Let $N = \text{int}[(R_d/T_{\min})]$ and $T = R_d/N$. If T is not an integer, the value of $(R_d \bmod N)$ is evenly distributed to the foremost $(R_d \bmod N)$ time steps in unit of 1 s. For example, if $R_d = 107$ s and $T_{\min} = 24$ s, then $N = 4$, $T = R_d/N = 26$ and $R_d \bmod N = 3$s. Then the length of the foremost 3 time steps will increase 1 s, respectively, and then we have $T_1 = T_2 = T_3 = 27$ s and $T_4 = 26$ s. Different values of n correspond to different values of N, which in turn results in different T and different T_i. The best green time of each phase and whether there exists a phase transition in this time step will be found out according to different T_i values.

l_1	l_2	δ_1	δ_2

Figure 2: Four gene positions per time period.

4.1. Chromosome Design. Suppose that the value of transition duration R_d is divided into N time steps. For each time step, it is necessary to determine whether phase transition exists, how many phase transitions have taken place (1 or 2 times) and the duration of the two phases. To express all of the information mentioned above, four gene bits need to be designed at each time step, as shown in Figure 2.

Where l_1 and l_2 represent the duration time of the first phase and second phase, respectively; the value of δ_1 (δ_2) is 1 or 0, where $\delta_1 = 1$ ($\delta_2 = 1$) indicates that there exists a signal transition from phase 1 (phase 2) to phase 2 (phase 1), and $\delta_1 = 0$ ($\delta_2 = 0$) otherwise. When expressed in this way, the values of δ_1 and δ_2 determine the subsequent phase. If $\delta_1 = 1$, then the subsequent phase can only be phase 2. Otherwise, the subsequent phase is still phase 1. Similarly, if $\delta_2 = 1$, the subsequent phase can only be phase 1, and phase 2 otherwise. Basing on this representation method, once crossover and mutation are performed, a large number of infeasible solutions will appear and the computational efficiency will be reduced greatly. For example, if the original values of the four gene bits are [15, 15, 1, 1], it indicates that the traffic signal will transfer to phase 2 after phase 1 has executed 15 s, and phase 2 will also execute 15 seconds, and then phase transition will occur again, namely traffic signal will transfer from phase 2 to phase 1 again. If mutation occurs and the values of four gene bits change to [15, 15, 0, 1], it means that phase transition does not occur after phase 1 has executed 15 s, and phase 2 will not execute correspondingly. But we can infer from the third gene that phase 2 still executes 15 s, which is inconsistent with the actual situation and thereby corresponds to an infeasible solution.

In order to avoid the occurrence of the above infeasible solutions, when design chromosome, we make each time step correspond to two gene bits. If the length of each time step is T and the transition duration R_d is divided into N time steps, then the length of each chromosome is $2N$. The two gene bits of each time step are expressed as ◻◪. The first gene is described by two quantities: the phase represented by this gene (phase 1 or phase 2) and the duration of the represented phase during this time step. The second gene is a flag indicating whether a phase transition occurs when the signal is transferred from the current time step to the next time step, and its value is 1 if a phase transition occurs and 0 otherwise. Since the value 1 or 0 is generated randomly, it can represent different situations.

4.2. Encoding. The concrete encoding method of this paper is shown in Figure 3. The transition duration R_d is divided into N

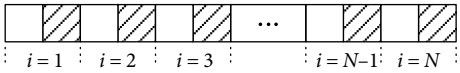

Figure 3: Real number encoding method.

time steps, and each time step $i, i = 1, 2, \ldots, N$ corresponds to two gene bits. Thus there are $2N$ gene bits in each chromosome. For the convenience of description, the positions of each gene bit of time step i in the whole chromosome are called the odd position and the even position of time step i. The odd position of time step i is described by two quantities, namely p_i and l_{i-pi} where p_i represents the corresponding phase and l_{i-pi} represents the duration time of the phase corresponding to p_i. It represents the first phase (phase 1) if $p_i = 0$ and the second phase (phase 2) if $p_i = 1$. If $l_{i-pi} > 0$, the value of l_{i-pi} may be the green time or the sum of the green time and the yellow time. Also, l_{i-pi} may be equal to 0. The even position of time step i is the flag bit, indicating whether there exists a phase transition or not, and it is described by δ_i. If $\delta_i = 1$, it indicates that phase transition occurs when traffic signal transfers from the current time step to the next time step, and $\delta_i = 0$ otherwise.

There are some restrictions on the duration of the phase represented by the first gene bit in each time period so as to ensure the feasibility of solution. Whether phase transition occurs during this time period can be implicitly denoted by the duration of the phase represented by the first gene bit. It is assumed in this paper that the EV passes through the intersection from west to east in the first phase, i.e., $p_1 = 0$. Generate the value of δ_1 randomly. If $\delta_i = 1$, it indicates that phase transition occurs from time step 1 to time step 2. If the first phase is performed all the time in the first time step, then $l_{1-p1} = T_1$. If phase switchover occurs in the first time period, namely the second phase is executed immediately after the first phase is executed, then the value of l_{1-p1} needs to ensure that the second phase can execute the minimum green time. If $\delta_1 = 0$, it means that phase transition from time step 1 to time step 2 does not occur, and the value of l_{1-p1} is unlimited as long as it does not exceed T_1.

For any $i > 1$, whether p_i represents the first phase or the second phase is related to all the quantities corresponding to the two gene bits in $i - 1$ time step, and it will be described in the following decoding process. Let $g_{\min}$ be the shortest green time of the first phase and the second phase, and Y be the yellow time of each phase. The value of l_{i-pi} is limited by δ_{i-1}. If $\delta_{i-1} = 1$, it means that the latest phase executed in time step $i - 1$ will be executed continuously in time step i, and the value of l_{i-pi} can be 0, T_i or between $[g_{\min} + Y,\ T_i - g_{\min} - Y]$. If $\delta_{i-1} = 0$, then it is similar to the first time step, and the value of l_{i-pi} is required to not exceed T_i.

4.3. Decoding

4.3.1. Determination of the Phase Represented by Odd Position of Each Time Period. Since it is deterministic that $p_1 = 0$ for the first time step, then the phase represented by p_2 can be determined directly. The chromosome shown in Figure 4 is taken as an example to illustrate the decoding idea of the phase represented by the odd position when $i = 2$. Figure 4

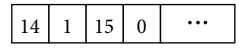

Figure 4: Example of normal chromosome.

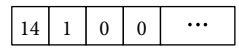

Figure 5: Example of special chromosome.

only shows the concrete value of each gene bit in the first two time steps by assuming $T_i = 30$ s, $i = 1, 2, \ldots, N$. Since $p_1 = 0$ and $l_{1-0} = 14$ s, it indicates that the first phase is executed for 14 s and then traffic light transfers to the second phase. We can indicate that $l_{1-1} = 30 - 14 = 16$ s, that is, the second phase is executed for 16 s. Since $\delta_1 = 1$, it indicates that phase transition occurs when transferring from time step 1 to time step 2, and the first phase will execute firstly in time step 2, namely $p_2 = 0$ and $l_{2-0} = 15$ s, indicating that after the first phase has been executed for 15 s the second phase will be executed continuously for $l_{2-1} = 30 - 15 = 15$ s. Since $\delta_2 = 0$, it indicates that phase transition does not occur when entering time step 3, that is, the second phase is executed continuously at the beginning of time step 3, and so on.

For the chromosome shown in Figure 4, if $l_{2-p2} = 0$ then it will be changed to Figure 5, and the result of decoding will be different. According to the values of the first two gene bits, the first phase will be executed firstly in time step 2, and the green time of the first phase should not be zero. But now $l_{2-p2} = 0$ means that the green time of this phase is 0 s. To avoid this obvious conflict, when decoding under this condition, it is obliged that $p_2 = 1$. That is, the odd position of time step 2 represents the second phase and $l_{2-1} = 0$. Therefore, the first phase is executed for 30 s namely $l_{2-0} = 30$. If $l_{2-p2} = 30$ s, it means that the green time of phase p_2 is equal to T_2, then $p_2 = 0$, $l_{2-0} = 30$ s and $l_{2-1} = 0$. Although both $l_{2-p2} = 0$ and $l_{2-p2} = 30$ s indicate that the first phase is executed for 30 s in time step 2, the phase represented by p_2 is different. Similarly, when $\delta_1 = 0$ or $l_1 = T_1$, a similar method can be used for analysis.

If $i > 2$, the phase corresponding to the odd position of the previous time step might be the first phase or the second phase. Therefore, when decoding it, the main work is to determine whether the phase corresponding to the odd position of the current time step is the same as that corresponding to the odd position of the previous time step. At this time, it can be analyzed in a similar way as $i = 2$.

4.3.2. Determination of the Green Time and Yellow Time of Each Phase. We can conclude from the knowledge mentioned above that the value of l_{i-pi} and $l_{i-(1-pi)}$ denote the green time of phase p_i and phase $1 - p_i$ in time step i or the sum of green time and yellow time. Since the green time and yellow time must be known clearly when calculating the two objective functions, it is necessary to determine whether the yellow time is included in l_{i-pi} and $l_{i-(1-pi)}$, which depends on the phase switchover in that time step. After the yellow time Y_{i-pi} of phase i and the yellow time $Y_{i-(1-pi)}$ of phase $i - 1$ have been determined, the green time of the two phases are also determined simultaneously. The green time of phase p_i and

phase $1 - p_i$ is $l_{i-pi} - Y_{i-pi}$ and $l_{i-(1-pi)} - Y_{i-(1-pi)}$, respectively. The green time of each phase is the value of decision variable $g_{j(k)}$.

Let α be the phase represented by the odd position of time step i. It is deterministic that $\alpha = 0$ for the first time step, and the value of α may be 0 or 1 for others. The calculation method of the yellow time of each phase in each time step is as follows.

(1) $0 < l_{i-pi} < T_i$

If $\delta_i = 1$, then phase transitions occur both in time step i and in the period from time step i to time step $i+1$, and both phases include yellow time. That is, $Y_{i-pi} = Y$ and $Y_{i-(1-pi)} = Y$; If $\delta_i = 0$, then phase transition occurs in time step i but not in the period from time step i to time step $i+1$, and yellow time is included only in phase p_i but not in phase $1 - p_i$, that is, $Y_{i-pi} = Y$ and $Y_{i-(1-pi)} = 0$.

(2) $l_{i-pi} = T_i$

If $\delta_i = 1$, then phase transition occurs in the period from time step i to time step $i+1$ but not in time step i, and yellow time is included only in phase p_i but not in phase $1 - p_i$. That is, $Y_{i-pi} = Y$ and $Y_{i-(1-pi)} = 0$; If $\delta_i = 0$, then phase transition does not occur both in time step i and in the period from time step i to time step $i+1$, and neither phase includes yellow time n, that is, $Y_{i-pi} = 0$ and $Y_{i-(1-pi)} = 0$.

(3) $l_{i-pi} = 0$

If $\delta_i = 1$ then phase transition occurs in the period from time step i to time step $i+1$ but not in time step i. Since $l_{i-(1-pi)} = T$, then yellow time is included only in phase $1 - p_i$ but not in phase p_i, that is, $Y_{i-pi} = 0$ and $Y_{i-(1-pi)} = Y$; If $\delta_i = 0$, then there is phase transition neither in time step i nor in the period from time step i to time step $i+1$, and neither phase includes yellow time, that is, $Y_{i-pi} = 0$ and $Y_{i-(1-pi)} = 0$.

4.4. Selection, Crossover and Mutation Operator

4.4.1. Selection Operator. Since there are more than one optimization objectives in a multi-objective optimization model, the selection method of single-objective optimization problem cannot be used for the selection operation of multi-objective optimization problem. Instead, the selection operation is performed by two steps: chromosome sorting and the same-level nondominated solution aggregation density sorting. Chromosome sorting is a ranking method based on the Pareto optimal concept. In this paper, an improved fast sorting method is adopted in chromosome sorting [31, 32].

The method of chromosome sorting makes it possible to preferentially select chromosomes with lower level to participate in evolution. It is also needed to determine a selection strategy for chromosomes with the same level so as to realize the selection operation of such chromosomes. In order to maintain the distribution and diversity of the evolutionary population, aggregation density strategy is adopted to select chromosomes with the same level. In the process of selecting chromosomes with the same level, chromosomes with small aggregation density are usually selected to participate in the next generation. Crowding distance is introduced to determine the aggregation density of chromosomes, and the chromosomes with larger crowding distance have a small aggregation density. Assume that chromosome i has r sub-targets, and $P[i]_{\text{distance}}$, the crowding distance of chromosome i is represented by the sum of the distances of the former chromosome $i-1$ and the latter chromosome $i+1$ on each sub-target. The calculation equation is:

$$P[i]_{\text{distance}} = \sum_{k=1}^{r} \left(P[i+1].f(k) - P[i-1].f(k)\right), \quad (17)$$

where $P[i].f(k)$ is the function value of the kth sub-target of chromosome i.

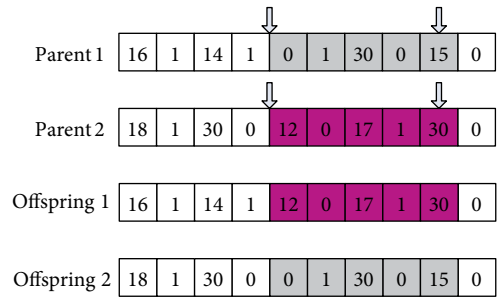

Figure 6: Partly matched crossover.

4.4.2. Crossover Operator. The partially matched crossover method is used in this paper for crossover [33]. First, two parent chromosomes are selected randomly according to the crossover probability and several gene bits are selected randomly from $2N$ gene bits of a pair of parent chromosomes. Then, the positions of the two groups of genes are exchanged. The concrete operation process is shown in Figure 6.

4.4.3. Mutation Operator. Randomly select a chromosome based on the mutation probability and generate two random integer numbers e, f from 1 to N, and exchange the values of the even position of the two gene bits. The specific operation process is shown in Figure 7.

4.5. Specific Flow of Algorithm. Now, the specific flow of NSGA-II algorithm adopted to find the control schemes is given as follows.

Step 1. Given the values of intersection parameters and traffic flow parameters such as ws_0, d_1, d_2, C, t_0, t_{safe}, $T_{\min}$; $g_{j\min}$ and $g_{j\max}$, $j = 1, 2$; A_{f-i}, S^i_{gf}, and S^i_{yf}, $i = t, r, l$, etc. Calculate the values of a and b according to formula (2), R_d according to formula (3), and N, T_i, $i = 1, 2, \cdots, N$ according to the method shown in Section 4.

Step 2. Initialize parameters of genetic algorithm such as population size, maximum number of iterations, crossover probability and mutation probability, and define chromosome structure.

Step 3. Create an initial population according to the method shown in Section 4.2 on the basis of the value of $g_{\min}$, N, and T_i, $i = 1, 2, \cdots, N$. Obtain the value of Y_{i-pi} and $Y_{i-(1-pi)}$

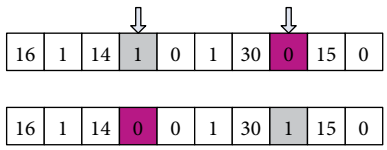

Figure 7: Mutation.

according to the value of δ_i, l_{i-pi} and $l_{i-(1-pi)}$ of the initial population, and then determine the value of decision variable $g_{j(k)}$ and $\alpha_{j(k)}$. Calculate values of the two objective functions of each chromosome.

Step 4. Sort the initial population with nondominated sorting method and calculate the crowding distance $P[i]_{\text{distance}}$ of each chromosome.

Step 5. Determine whether the current number of iterations is greater than the maximum number of iterations. If it is, output the current Pareto-optimal solutions and end the algorithm; otherwise, go to Step 6.

Step 6. Select chromosomes by binary tournament selecting method to take-on crossover operation according to the crossover probability, generate offspring chromosomes and calculate values of the two objective function of each offspring chromosome.

Step 7. Select chromosomes by binary tournament selecting method to mutate their structures according to the mutation probability, and calculate values of the two objective functions of each mutated chromosome.

Step 8. Combine offspring and parent populations together, calculate crowding distance $P[i]_{\text{distance}}$ of each chromosome and sort all the chromosomes according to each chromosome's values of the two objective functions and crowding distance.

Step 9. Cut the combined population to a given number according to the sorting results, sort the population after cutting with nondominated sorting method and calculate crowding distance $P[i]_{\text{distance}}$ of each chromosome.

Step 10. Record the current Pareto-optimal solutions, add 1 to the current number of iterations and go to Step 5.

5. Simulation Analyses

Assume that the EV passes through the intersection from west to east. For the base case, namely normal operation, the following signal timing was used. Cycle time $C = 84$s; the green time of phase 1 and phase 2 is 50 s and 30 s, respectively; the yellow time is 2 s for both phases; the starting time of the first phase $ws_0 = 0$ s; $d_1 = 52$ s, $d_2 = 32$ s, $t_{\text{safe}} = 2$ s; $g_{1\min} = g_{2\min} = 10$ s, $g_{1\max} = g_{2\max} = 60$ s, $T_{\min} = 24$ s; $S^t_{gf} = 0.5\,\text{pcu}\cdot\text{s}^{-1}$, $S^r_{gf} = 0.95S^t_{gf}$, $S^l_{gf} = 0.85S^t_{gf}$, $S^t_{yf} = 0.25\,\text{pcu}\cdot\text{s}^{-1}$, $S^r_{yf} = 0.95S^t_{yf}$, $S^l_{yf} = 0.85S^t_{yf}$, $f = 1, 2, 3, 4$; Turning movement ratios are set to 20%, 70%, and 10% for right, through, and left turns, respectively in west-east and east-west direction, and 30%, 60%, and 10% in north-south and south-north direction.

The NSGA-II algorithm was run for 200 generations in all cases. The control parameters used in the NSGAII -based optimization process are as follows

(i) Population size: 100;
(ii) Crossover probability: 0.8;
(iii) Mutation probability: 0.02;
(iv) Number of generations: 200.

In this paper, we defined four scenarios. The time t_0 at which EV passed through the intersection was set to 8 o'clock, 9 o'clock, 10 o'clock, and 18 o'clock, respectively, and runs for each scenario were simulated. In different scenarios, EV passed through the given intersection in the first or the second phase of the background cycle, and the elapsed green time of the first or the second phase of the background cycle for each scenario was different.

When t_0 is 9 o'clock or 10 o'clock, we assume the initial queue lengths of straight, right-turn and left-turn for west-east and east-west direction are 10, 8, and 6, respectively, and 8, 7, and 6, respectively for north-south and south-north direction. The arrival rate is a random variable and it is 1440–1800 pcu/h for west-east and east-west direction and 1260–1440 pcu/h for north-south and south-north direction. The Pareto solution set of different number of additional normal cycle (n) for 9 o'clock is shown in Figure 8.

We can see from Figure 8 that corresponding to different n the number of time step N is different when t_0 is 9 o'clock and this conclusion is applicable to other time as well. The number of the Pareto solutions is 5, 3, and 3 respectively for one, two and three additional normal cycles, and the green time of phase 1 and phase 2 for different Pareto solution is also different.

The Pareto frontier with different n for 9 o'clock and 10 o'clock are shown in Tables 1 and 2. The final Pareto frontier for 9 o'clock and 10 o'clock are shown in Figures 9 and 10.

As can be seen from Tables 1 and 2 that, for each solution with different n in the Pareto solution set, with the reduction of one objective, the other objective is reduced simultaneously, which implies that the decrease in the difference between the maximum queue length and the minimum queue length in all directions (f_2) is at the cost of the reduction of the number of vehicles passing through the intersection per unit time during the transition period (f_1). From Figures 9 and 10 we can conclude that, the Pareto frontier is composed of nondominant solutions selected from all Pareto solutions corresponding to different n. In the six Pareto solutions shown in Figure 9, three solutions come from $n = 1$, two solutions come from $n = 2$ and only one solution comes from $n = 3$. What is more, the solutions for $n = 1$ and $n = 2$ appear alternately, while the two objectives of the solution from $n = 3$ are smaller than those of $n = 1$ and $n = 2$. Unlike the results in Figure 9, the solutions in Figure 10 show that a larger n corresponds to a smaller difference between the maximum queue length and the minimum queue length in all directions, while a smaller n has a bigger number of vehicles passing through the intersection per unit time. The difference between Figures 9 and 10 tells us that if EV passes through the intersection in different phases of the background cycle or it passes through the intersection

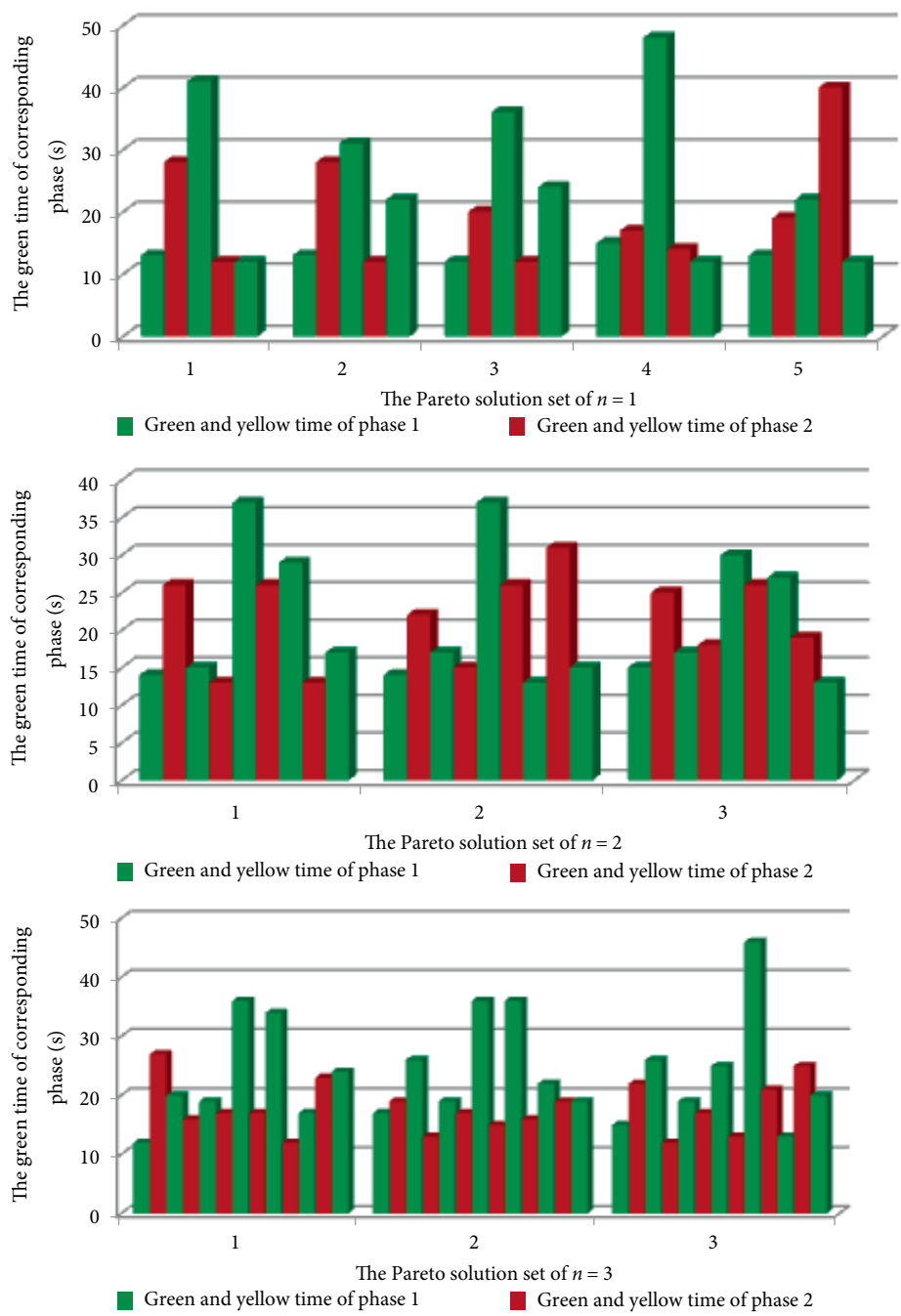

Figure 8: Pareto solution set corresponding to different n for 9 o'clock.

in the same phase but the elapsed green time of this phase is different, the Pareto solutions with different n will be diverse, correspondingly.

To verify the control effect of the transition method presented in this paper under the condition of much larger traffic volume, we assume that 8 o'clock is the morning peak period and 18 o'clock is the evening peak period. Suppose that for both periods the arrival rate is 1980–2160 pcu/h for west-east and east-west direction and 1800–1980 pcu/h for north-south and south-north direction, respectively. The initial queue lengths in all directions are doubled compared with the initial queue length at 9 o'clock and 10 o'clock. The Pareto optimal set of the morning peak period (8 o'clock) and of the evening peak period (18 o'clock) is shown in Tables 3 and 4, respectively.

From Tables 3 and 4, we can infer that although there are many queued vehicles at each direction and the arrival rate exceeds the saturation flow rate, the signal transition method can still guarantee both fair and efficiency, which is embodied in the smaller difference of the queue length in all directions and the larger number of vehicles passing through the intersection in unit time. Also we can conclude that if we want to have larger passing through vehicles in unit time, we can choose to add one additional normal cycle. Adding two or

Table 1: Pareto frontier with different n when t_0 is 9 o'clock.

Corresponding cycle	f_1 (pcu/s)	f_2 (pcu)
	2.71	5.1
	2.64	4.5
$n = 1$	2.60	3.8
	2.57	2.7
	2.25	1.8
	2.69	6.2
$n = 2$	2.67	4.5
	2.59	3.3
	2.59	4.7
$n = 3$	2.52	2.8
	2.45	1.1

Table 2: Pareto frontier with different n when t_0 is 10 o'clock.

Corresponding cycle	f_1 (pcu/s)	f_2 (pcu)
	2.73	6.2
	2.63	3.6
$n = 1$	2.31	2.1
	2.30	1.7
	2.27	0.2
	2.62	6.1
$n = 2$	2.57	3.0
	2.39	1.9
	2.52	3.4
$n = 3$	2.49	1.9
	2.45	0.0

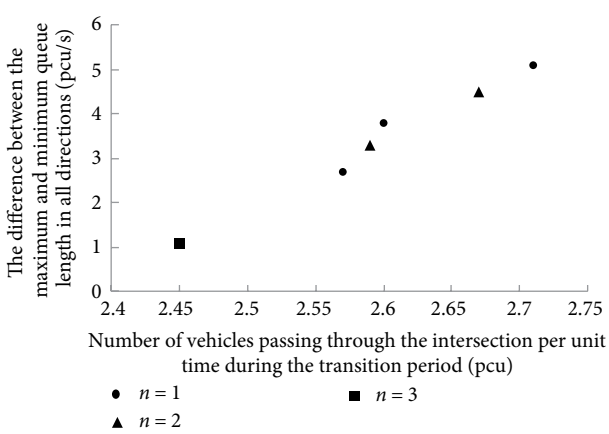

Figure 9: Pareto frontier when t_0 is 9 o'clock.

three additional normal cycle is suitable for obtaining smaller difference of queue length in all directions. The results shown in Tables 3 and 4 also indicate that the signal preemption control method is effective when the arrival rate is much larger in the morning peak period.

To check the effectiveness of the control strategy of EV signal transitioning from EVSP back to normal operation presented in this paper, comparison work between this control strategy and traditional classical transition method named smooth transition is carried out. Simulations of smooth

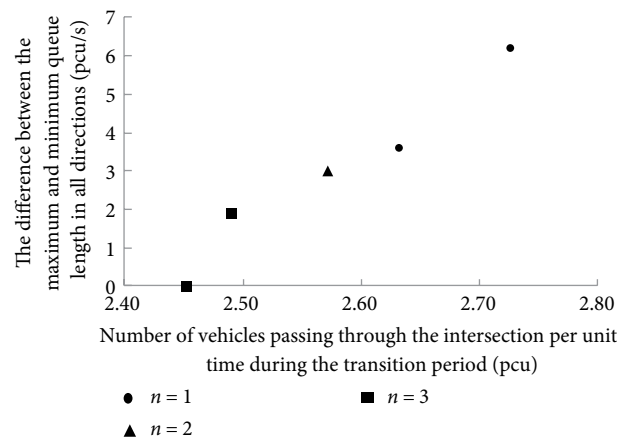

Figure 10: Pareto frontier when t_0 is 10 o'clock.

Table 3: Pareto frontier of the morning peak period.

Number	f_1 (pcu/s)	f_2 (pcu)	Corresponding n
1	2.80	8.1	1
2	2.72	7.0	1
3	2.70	6.2	1
4	2.64	5.2	1
5	2.83	10.4	2
6	2.57	4.3	2
7	2.56	4.1	3
8	2.53	3.0	3

Table 4: Pareto frontier of the evening peak period.

Number	f_1 (pcu/s)	f_2 (pcu)	Corresponding n
1	2.79	8.0	1
2	2.66	7.7	1
3	2.61	6.3	1
4	2.59	5.8	1
5	2.57	5.4	1
6	2.51	3.5	2
7	2.36	2.7	3

transition control method under each of the given four scenarios are executed 20 runs respectively, and the simulation results are shown in Table 5. The results of Pareto frontier with the worst f_1 (but the best f_2), and the worst f_2 (but the best f_1) at each time point obtained by this method are also listed in Table 5.

It can be concluded from Table 5 that there is little difference in the number of vehicles passing through the intersection in unit time obtained by the two methods, and the results with the best f_1 (the worst f_2) are superior to the average f_1 obtained by smooth transition method in all scenarios. But there is obvious disparity in the difference of queue length obtained by the two methods. The difference of queue length obtained by smooth transition method is obviously larger than that obtained by the method presented in this paper, and the difference is especially large during the morning and evening peak period

Table 5: Simulation results of smooth transitioning control method.

Time	This method with the worst f_1 (the best f_2)		This method with the worst f_2 (the best f_1)		Smooth transition	
	f_1 (pcu/s)	f_2 (pcu)	f_1 (pcu/s)	f_2 (pcu)	f_1 (pcu/s)	f_2 (pcu)
8 o'clock	2.53	3.0	2.80	8.1	2.76	27.3
9 o'clock	2.25	1.8	2.69	6.2	2.03	14.9
10 o'clock	2.27	0.2	2.62	6.1	1.87	16.4
18 o'clock	2.36	2.7	2.79	8.0	2.75	25.5

because of the large traffic volume. Compared with the average value of f_2 obtained by smooth transition method, the shorten rates of the worst f_2 at each time point obtained by this method is 70.33%, 58.39%, 62.80% and 68.63%, respectively. Therefore, the proposed signal transition method can give consideration to both efficiency and fairness of each direction.

When more than one EV arrives, the signal transition method proposed in this paper is also applicable. If the arrival interval of adjacent EV is relatively long, traffic signal can be transferred to normal operation as long as each EV passing through the intersection by adopting this method. If the arrival interval of adjacent EV is very short, they can be seen as one EV and signal transition will not be carried out until they have both passed through the intersection.

6. Conclusions

Control strategy of EV signal transitioning from EVSP back to normal signal timing scheme was discussed in this paper. A multi-objective transition optimization model was presented considering both efficiency and fairness, and a solving method based on nondominated sorting genetic algorithm II was designed to solve the optimization model. In order to avoid a large number of infeasible solutions in the algorithm and considering the nature of the problem, we designed a unique chromosome structure and put forward special encoding and decoding methods.

Simulation was carried out in this paper to verify the control effect of the proposed strategy, and the value of the two objectives was calculated. The Pareto solution set of different number of additional normal cycle and the Pareto frontier for different scenarios was obtained. The data were compared with those obtained by smooth transition method. The results show that the control strategy obtained by the multi-objective programming model in this paper is superior to that obtained by smooth transition method in all cases.

We assume that the arrival rate is a random variable in this paper. But perhaps the distribution function of arrival rate under emergency events is not close enough to the frequency. Since the arrival rate has some influence on the stability of control strategy, future research will focus on signal transition strategy under this condition and study it in uncertainty environments.

Data Availability

The data used to support the findings of this study are available from the corresponding author upon request.

Conflicts of Interest

The authors declare that they have no conflicts of interest.

Acknowledgments

This research is supported by National Nature Science Foundation of China (Nos. 61563029, 71671079, 71361018, and 71571090) and National Key R&D Program of China (No. 2018YFB1201602).

References

[1] Federal Highway Administration (FHWA), "Traffic signal preemption for emergency vehicles: a cross-cutting study," 2006, http://www.its.dot.gov.

[2] A. Shrivastava, S. Rawat, H. K. Singh, K. Neelam, D. Prasad, and V. Nath, "Preemption of traffic signal using global positioning system (GPS)," in *Proceedings of the Third International Conference on Microelectronics, Computing and Communication Systems*, Springer, Singapore, 2019.

[3] J. Yao, K. Zhang, Y. Yang, and J. Wang, "Emergency vehicle route oriented signal coordinated control model with two-level programming," *Soft Computing*, vol. 22, no. 13, pp. 4283–4294, 2018.

[4] J. Wang, X. Yang, and W. Ma, "Development of degree-of-priority based preemption control strategy for emergency vehicle operation," *Transportation Research Board 92nd Annual Meeting*, vol. 69, pp. 7215–7227, 2013.

[5] X. Li, W. Pu, and X. Zhao, "Agent action diagram: toward a model for emergency management system," *Simulation Modelling Practice and Theory*, vol. 94, pp. 66–99, 2019.

[6] S. Singh, "Utility dependency reduction by multi-agent participation in smart grid," *Advances in Systems Science and Applications*, vol. 19, no. 2, pp. 90–100, 2019.

[7] K. H. Chen, C. R. Dow, C. W. Yang, and W. C. Chiang, "BEVOR: an NTCIP-based interoperable framework for emergency vehicle preemption system using web service and STMF," *Journal of Information Science & Engineering*, vol. 26, no. 3, pp. 801–815, 2010.

[8] S. Humagain, R. Sinha, E. Lai, and P. Ranjitkar, "A systematic review of route optimization and pre-emption methods for emergency vehicles," *Transport Reviews*, pp. 1–19, 2019.

[9] Y. S. Huang, Y. S. Weng, and M. C. Zhou, "Design of traffic safety control systems for emergency vehicle preemption using timed petri nets," *IEEE Transactions on Intelligent Transportation Systems*, vol. 16, no. 4, pp. 2113–2120, 2015.

[10] H. Ong, *Emergency Vehicle Pre-Emption (EVP): A Review with a Case Study on Brisbane EVP*, Queensland University of Technology, Brisbane, Australia, 2019.

[11] E. Nelson and D. Bullock, *Impact Evaluation of Emergency Vehicle Preemption on Signalized Corridor Operation: An Evaluation, Transportation Research Record 1727*, pp. 1–11, TRB, Washington, DC, USA, 2000.

[12] S. Shelby, D. Bullock, and D. Gettman, *Transition Methods in Traffic Signal Control, Transportation Research Record 1978*, pp. 130–140, TRB, Washington, DC, USA, 2006.

[13] D. Cohen, L. Head, and S. Shelby, "Performance analysis of coordinated traffic signals during transition," *Transportation Research Record: Journal of the Transportation Research Board*, vol. 2035, no. 1, pp. 19–31, 2007.

[14] T. Pohlmann and B. Fiedrich, "Traffic signal transition in coordinated meshed networks," *Transportation Research Record: Journal of the Transportation Research Board*, vol. 2192, no. 1, pp. 97–107, 2010.

[15] C. Hamliton, *Evaluation of Traffic Signal Controller Transition Methods*, Texas A&M University, Texas, TX, USA, 2012.

[16] E. Lieberman and D. Wicks, *A Rapid Signal Transition Algorithm, Transportation Research Record 505*, pp. 1–15, TRB, Washington, DC, USA, 1974.

[17] Z. Zhang, Q. He, J. Gou, and X. Li, "Analyzing travel time reliability and its influential factors of emergency vehicles with generalized extreme value theory," *Journal of Intelligent Transportation Systems*, vol. 23, no. 1, pp. 1–11, 2019.

[18] W. Min, Y. Liang, C. Peng, M. Zhang, Y. Liu, and J. Wang, "On-demand greenwave for emergency vehicles in a time-varying road network with uncertainties," *IEEE Transactions on Intelligent Transportation Systems*, pp. 1–13, 2019.

[19] J. Lee and B. M. Williams, "Development and evaluation of a constrained optimization model for traffic signal plan transition," *Transportation Research Part C: Emerging Technologies*, vol. 20, no. 1, pp. 185–198, 2011.

[20] H. F. Guo, Q. T. Peng, and J. Cheng, "A novel method for fast smoothing transition of arterial coordination control plans," *Journal of Southwest Jiaotong University*, vol. 49, no. 5, pp. 882–887, 2014.

[21] K. Shaaban, M. A. Khan, R. Hamila, and M. Ghanim, "A strategy for emergency vehicle preemption and route selection," *Arabian Journal for Science and Engineering*, vol. 44, no. 10, pp. 8905–8913, 2019.

[22] A. B. Shu, L. Y. Zhang, and L. Xu, "Transition adjustment tactic of signal coordinated control scheme for urban traffic arterial," *Traffic Information and Safety*, vol. 33, no. 1, pp. 122–126, 2015.

[23] M. Selekwa and A. Chiteshe, "Development of an optimal timing plans' transition procedure," *Transportation Research Record: Journal of the Transportation Research Board*, vol. 12, no. 2, pp. 20–25, 2002.

[24] E. C. Chang, "Signal transition interval for computerized traffic signal systems," *Transportation Planning Journal*, vol. 16, no. 3, pp. 527–553, 1987.

[25] J. Obenberger and J. Collura, *Methodology to Assess Traffic Signal Transition Strategies for Exit Preemption Control, Transportation Research Record 2035*, pp. 158–168, TRB, Washington, DC, USA, 2007.

[26] I. Yun, M. Best, and B. Park, "Evaluation of emergency vehicle preemption strategies on a coordinated actuated signal system using hardware-in-the-loop simulation," *ASCE Journal of Transportation Engineering*, vol. 134, no. 10, pp. 423–431, 2008.

[27] X. Qin and A. M. Khan, "Control strategies of traffic signal timing transition for emergency vehicle preemption," *Transportation Research Part C: Emerging Technologies*, vol. 25, no. 25, pp. 1–17, 2012.

[28] J. Yao, K. Zhang, Y. Dai, and J. Wang, "Power function-based signal recovery transition optimization model of emergency traffic," *The Journal of Supercomputing*, vol. 74, no. 12, pp. 7003–7023, 2018.

[29] K. Deb, S. Agrawal, and A. Pratap, *A Fast Elitist Nondominated Sorting Genetic Algorithm for Multi-Objective Optimization: NSGA II, Parallel Problem Solving from Nature (PPSN VI)*, Springer, Berlin, 2000.

[30] J. Liu and X. Chen, "An improved NSGA-II algorithm based on crowding distance elimination strategy," *International Journal of Computational Intelligence Systems*, vol. 12, no. 2, pp. 513–518, 2019.

[31] J. Zheng, *Multiobjective Evolutionary Algorithms and Their Applications*, Science Press, China, 2010.

[32] S. Foroughi, J. K. Hamidi, M. Monjezi, and M. Nehring, "The integrated optimization of underground stope layout designing and production scheduling incorporating a nondominated sorting genetic algorithm (NSGA-II)," *Resources Policy*, vol. 63, p. 101408, 2019.

[33] Y. Zheng, X. Lu, M. Zhang, and S. Chen, *Optimization Problems and Algorithms: Biogeography-Based Optimization: Algorithms and Applications*, Springer, Singapore, 2019.